BULLETIN OF THE POLISH ACADEMY OF SCIENCES
TECHNICAL SCIENCES, Vol. 61, No. 2, 2013
DOI: 10.2478/bpasts-2013-0038

Method for stabilogram characterization using angular-segment function

J. FIOŁKA* and Z. KIDOŃ

Institute of Electronics, Silesian University of Technology, 16 Akademicka St., 44-100 Gliwice, Poland

Abstract. This paper presents a new approach to descriptions of stabilograms. In the proposed method, a one-dimensional angular-segment function is generated from the stabilographic trajectory data. This allows to reduce the data dimensionality and makes the analysis easier. Moreover, three methods of angular-segment function parameterization are also presented in this study. The obtained results confirm the usefulness of the proposed parameters for medical diagnoses.

Key words: posturography, biomedical signal analysis, signal processing.

1. Introduction

Posturography is a unique clinical assessment technique that is used to analyze human postural stability [1, 2]. In static posturography, a patient stands in an upright position on a stationary force test platform. During the trial time, which lasts from 30 to 120 seconds, the ground reaction forces, generated by the subject, are continuously registered. Then, with the aid of elementary Newtonian mechanics, these forces are used to calculate the coordinates T_i ($x[i]$, $y[i]$) of the center of pressure (CoP) over the platform surface. A plot of the time-varying coordinates of the CoP is known as a stabilogram or, sometimes, as a posturographic/stabilographic trajectory. As an example, Fig. 1 shows the CoP trajectory of a healthy person along with its individual components, in the anterior-posterior (AP) and medial-lateral (ML) directions.

Today, static posturography is used widely in the evaluation of the human balance system. It allows the relationships that exist among all of the components of the human balance system to be examined (the human balance system consists of three distinct systems that work together – the Vestibular, the Visual and the Somatic Sensory System). A comprehensive study of the biomechanical models of balance with an emphasis on the fundamental issues can be found in [3]. It should be also noted that many authors have investigated the relationship between balance disorders and the properties of stabilographic trajectories [4, 5]. Moreover, in recent years much attention has been paid to the application of static posturography in the field of rehabilitation e.g. to the diagnosis of posture defects, postural re-education and the assessment of rehabilitation progress [6–8].

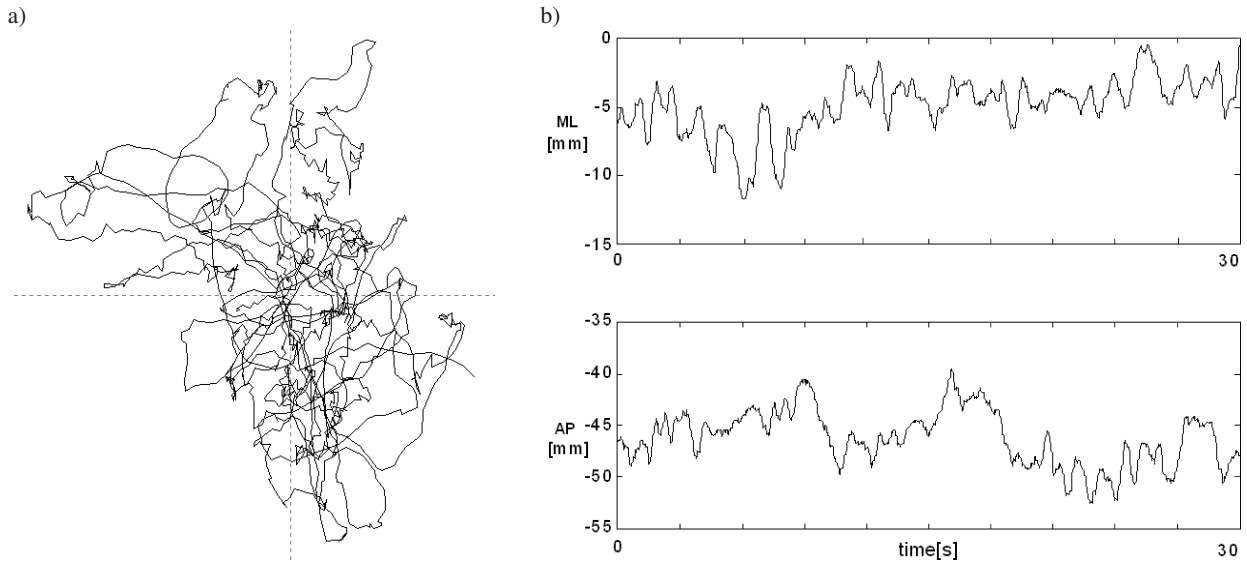

Fig. 1. An example of a stabilogram (a) and its components (b)

*e-mail: jerzy.fiolka@polsl.pl

2. Cumulative angular-segment function

For the diagnosis of some skeletal diseases, the CoP trajectory shape is more significant than its size. In order to make the comparison of trajectory shapes and the analysis easier, a one-dimensional function describing the trajectory curve has been developed. The proposed cumulative angular-segment function (*ASF*) was inspired by the cumulative angular function used for the recognition and classification of closed curves. The overall length of a closed curve (e.g. a cell contour) is divided into N parts by marking N equally-spaced points on it. Starting from zero, the successive values of the cumulative angular function are obtained by calculating the differences between the inclination angle values of the vectors corresponding to the successive points marked on the curve and then adding those differences up. At the end of the contour, after returning to the starting point, we get the cumulative angular function value equal to 2π. Assuming that the sampling of the successive function values runs at a constant rate and is not limited to a single cycle, we get the periodical cumulative angular function. After the Fourier expansion of that function, we get the amplitudes and phases of harmonics, which can be applied for the classification of the trajectory shape, irrespective of its size [9].

Although the stabilographic trajectory is an open and discrete-time curve, the trajectory cumulative angular function still contains information about the trajectory shape. The distances between the following T_i ($x_T[i]$, $y_T[i]$) measured points of the original CoP trajectory depend on the body sway speed and they differ from each other. In order for the trajectory shape to be reproduced by the cumulative angular function, it is necessary for the distances between the successive trajectory points to be constant. Therefore, the cumulative angular function cannot be calculated directly from the original trajectory points. The equally-spaced points must first be appointed on the original trajectory and the so-called recalculated trajectory has to be defined in this manner.

Two algorithms for converting the original trajectory into the recalculated one were developed. The distance or path length L (along the original trajectory) between each of two consecutive points K_j ($x_K[j]$, $y_K[j]$) and K_{j+1} ($x_K[j+1]$, $y_K[j+1]$) of the recalculated trajectory is constant. The recalculated trajectory has the same shape as the original one. In order to compare only the trajectory shapes and not their sizes, the distance L should be derived from the original trajectory length (*TL*) using the following formula:

$$L = TL/N, \tag{1}$$

where N – number of recalculated trajectory points (usually equal to the number of the original trajectory points).

2.1. Cumulative angular-segment function *ASF*α with a constant distance between the recalculated consecutive trajectory points. The cumulative angular-segment function *ASF*α was defined for the constant distance L between the consecutive points of the recalculated trajectory. The formula (2) presents the discrete angular increments of *ASF*α.

$$\begin{cases} ASF\alpha[1] = 0 \\ ASF\alpha[j+1] = ASF\alpha[j] + \Delta\alpha[j] \quad \text{for } j = 1, 2, 3 \ldots \end{cases} \tag{2}$$

While moving from one point to another, the trajectory can turn right or left. The discrete angular increment satisfies the inequality $0 < \Delta\alpha[j] < \pi$ when the trajectory "turns left" and $-\pi < \Delta\alpha[j] < 0$ when the trajectory "turns right". The trajectory can turn many times in the same direction. As a result, the *ASF*α function values are not limited to the range of [0..2π). The $\Delta\alpha[j]$ increment can be calculated using the following formulas:

$$\begin{cases} \Delta\alpha[j] = \alpha^*[j+1] - \alpha[j] & \text{for } \alpha^*[j+1] - \alpha[j] \le \pi \\ \Delta\alpha[j] = \alpha^*[j+1] - \alpha[j] - 2\pi & \text{for } \alpha^*[j+1] - \alpha[j] > \pi \end{cases}$$

where

$$\begin{cases} \alpha^*[j+1] = \alpha[j+1] & \text{for } \alpha[j+1] \ge \alpha[j] \\ \alpha^*[j+1] = \alpha[j+1] + 2\pi & \text{for } \alpha[j+1] < \alpha[j] \end{cases} \tag{3}$$

For example, when $\alpha[j] = 0.1\pi$ and $\alpha[j+1] = 1.8\pi$, $\Delta\alpha[j] = -0.3\pi$. The angle $\alpha[j+1]$ with the value in the range from 0 to 2π is the angle between the x-axis and the vector connecting the two successive points of the recalculated trajectory:

$$\begin{cases} \alpha[1] = 0 \\ \alpha[j+1] = \angle\left(0x, \overrightarrow{K_jK_{j+1}}\right) \quad \text{for } j = 1,\ 2,\ 3 \ldots \end{cases} \tag{4}$$

Points K_j and K_{j+1} of the recalculated trajectory lie on the original trajectory and the distance (L) between them is constant. Depending on the value L and the distance between the successive points of the original trajectory, the points K_j and K_{j+1} can either lie or not lie on the same segment of the original trajectory. For example, if the point K_j lies on the i-th segment of the original trajectory, the point K_{j+1} can lie on the i-th or the i+1-th or the i+2-th ... segment.

The coordinates of the points K_j and K_{j+1} should satisfy the following conditions:

$$\begin{gathered} K_j \in S_i, \quad K_{j+1} \in r(K_j, L) \cap S_n, \\ n = \min\left\{k : k \ge i,\ S_k \cap r(K_j, L) \ne \emptyset\right\}, \end{gathered} \tag{5}$$

where $L = dist(K_j, K_{j+1})$ is the distance between the points K_j and K_{j+1}, S_i is the i-th segment of the original trajectory connecting the points T_i and T_{i+1}, S_k is the k-th segment of the original trajectory ($k \ge i$) connecting the points T_k and T_{k+1}, $r(K_j, L)$ is the circle with the center at the point K_j and the radius L.

Sometimes two points satisfy the formula (5). In this case, the point K_{j+1} is chosen as that, whose distance to the original trajectory point T_k is smaller.

The developed algorithm processes the original trajectory point coordinates in a sequential way starting from the first one. Two cases are possible. The current and next points of

the recalculated trajectory (K_j and K_{j+1}) lie (Fig. 2b) or do not lie (Fig. 2a) on the same segment connecting two consecutive points (T_i and T_{i+1}) of the original trajectory. Figure 2c shows both a part of the recalculated trajectory and the original trajectory for the distance value L equal to the mean value of the distances between each consecutive pair of the original trajectory points.

As an example, Fig. 3 shows the $ASF\alpha$ characteristic of a healthy subject and a subject who has some disturbances of balance.

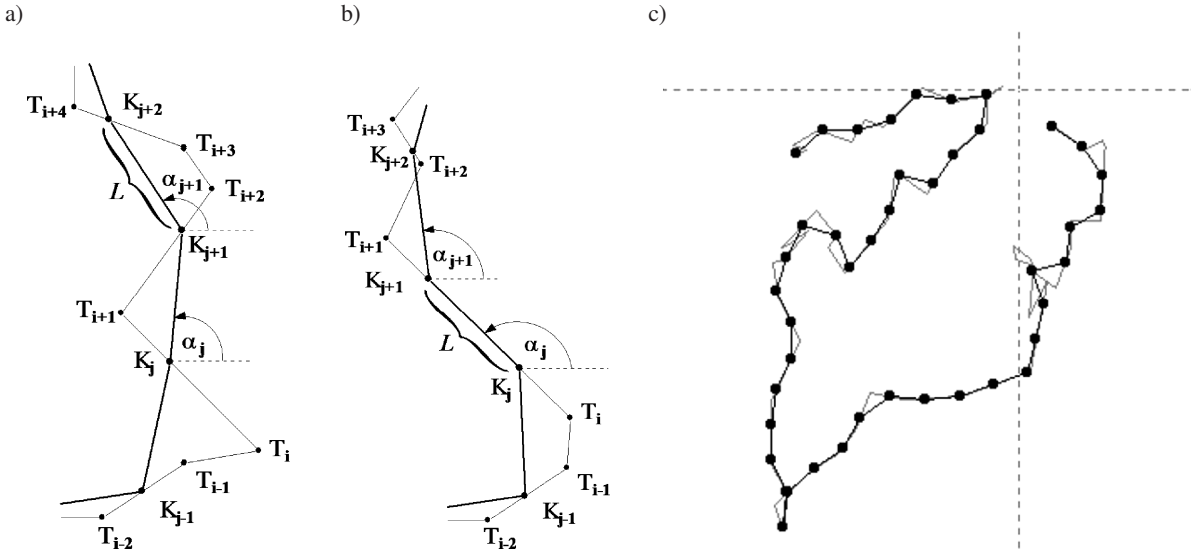

Fig. 2. Graphical illustration of the function $ASF\alpha$ calculation – points K_j, K_{j+1} of the recalculated trajectory lie (b) or do not lie (a) on the same original trajectory segment; (c) an example of the recalculated trajectory and the original one

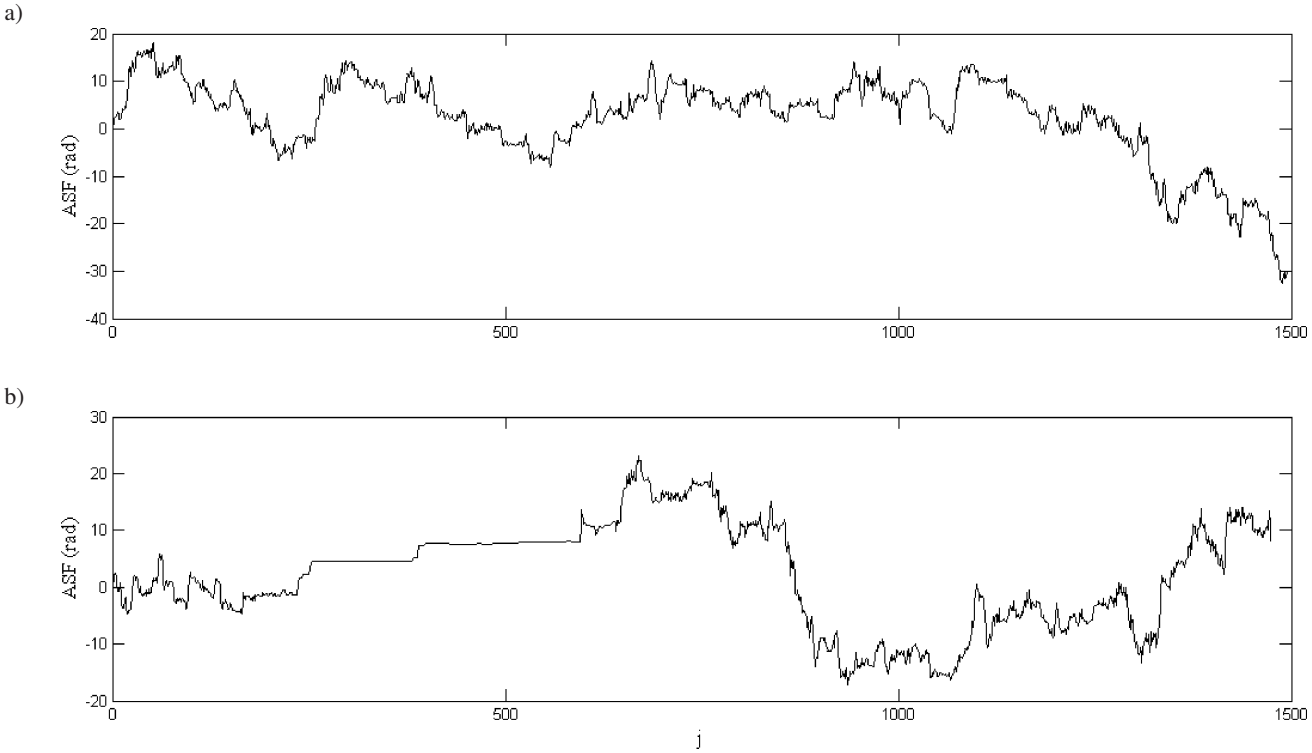

Fig. 3. The $ASF\alpha$ obtained from a healthy subject (top) and from a subject who has some disturbances of balance (bottom)

2.2. Cumulative angular-segment function *ASF*β with a constant path length between the recalculated consecutive trajectory points. The definition of the cumulative angular-segment function *ASF*β calculated for a constant path length L (measured along the original trajectory) between the recalculated consecutive trajectory points is identical to the *ASF*α definition – the angle $\alpha[j]$ should only be replaced with the angle $\beta[j]$ in formulas (2), (3) and (4). However, the algorithm that converts the original trajectory into the recalculated one is different. Now, the distance between recalculated consecutive trajectory points is not constant (as it was for *ASF*α); however, their path length L measured along the original trajectory is constant. For example, if the point K_j lies on the original trajectory between the points T_i and T_{i+1} and L is smaller than the distance between the points K_j and T_{i+1}, the point K_{j+1} will lie between T_i and T_{i+1}. Otherwise, the value of $dist(K_j, T_{i+1})$ has to be increased by the value of $dist(T_{i+1}, T_{i+2})$ and if this sum is bigger than L, the point K_{j+1} will lie between the points T_{i+1} and T_{i+2}. If the sum mentioned above is still smaller than L, it will be increased by the length of the successive segment of the original trajectory.

So K_j and K_{j+1} point coordinates can be calculated from the following equations:

$$\begin{cases} \begin{cases} dist\,(K_j, K_{j+1}) = L\,; \quad n = i \\ \quad \text{for} \\ \quad L \le dist\,(K_j, T_{i+1}) \end{cases} \\ \begin{cases} dist\,(K_j, T_{i+1}) + dist\,(T_{i+1}, K_{j+1}) = L\,; \quad n = i+1 \\ \quad \text{for} \\ \quad dist\,(K_j, T_{i+1}) < L \le dist\,(K_j, T_{i+1}) + dist\,(T_{i+1}, T_{i+2}) \end{cases} \\ \vdots \\ \begin{cases} dist\,(K_j, T_{i+1}) + \sum_{l=1}^{m} dist\,(T_{i+l}, T_{i+l+1}) \\ \qquad + dist\,(T_{i+m+1}, K_{j+1}) = L; \quad n = i+m+1 \\ \quad \text{for} \\ \quad dist\,(K_j, T_{i+1}) + dist\,(T_{i+1}, T_{i+2}) \\ \qquad < L \le dist\,(K_j, T_{i+1}) + \sum_{l=1}^{m+1} dist\,(T_{i+l}, T_{i+l+1}) \end{cases} \\ K_j \in S_i, \;\; K_{j+1} \in S_n \end{cases} \tag{6}$$

where $j = 1, 2, ...,$ is an index of the successive point K_j of the recalculated trajectory, $i = 1, 2, ...,$ is an index of the successive point T_i of the original trajectory, S_i is the i-th segment of the original trajectory connecting the points T_i and T_{i+1}, S_n is the n-th segment of the original trajectory ($n \ge i$) connecting the points T_n and T_{n+1}, m is the number of complete segments of the original trajectory included in the path L between one recalculated trajectory point and another.

Figure 4 shows two possible cases for the processing algorithm. The current and next points of the recalculated trajectory (K_j and K_{j+1}) lie (Fig. 4b) or do not lie (Fig. 4a) on the same segment connecting two consecutive points (T_i and T_{i+1}) of the original trajectory. Figure 4c shows a part of the recalculated trajectory and the original one.

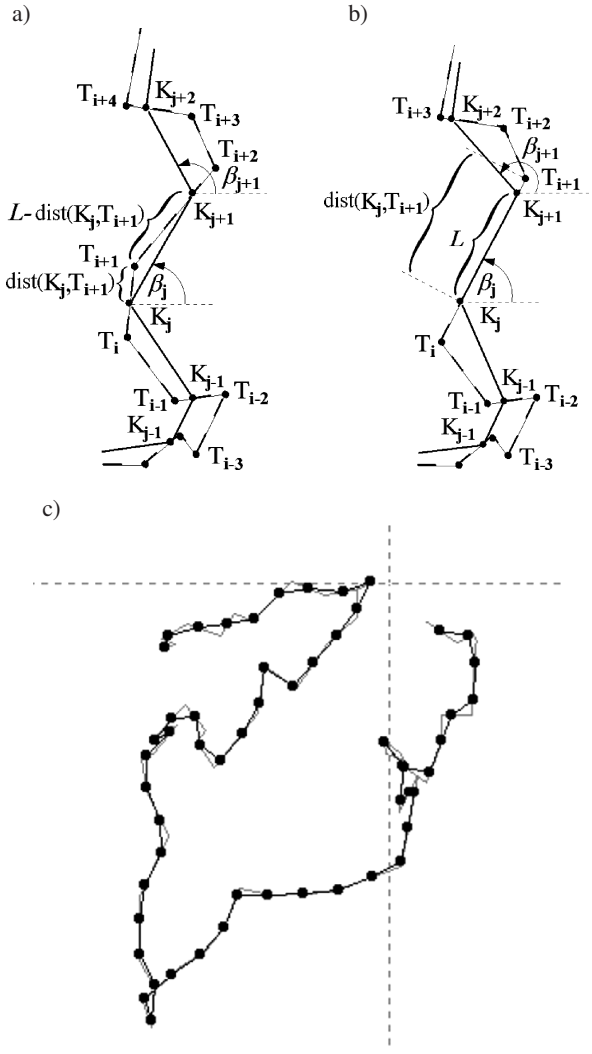

Fig. 4. Graphical illustration of the function *ASF*β calculation – points K_j, K_{j+1} of the recalculated trajectory lie (b) or do not lie (a) on the same original trajectory segment; (c) an example of the recalculated trajectory and the original one

The posturographic examinations carried out on three groups (see Sec. 4) allow us to formulate some conclusions concerning the properties of the angular-segment function. In studies of healthy subjects, the signal shows a relatively low variability between subjects. Moreover, similar, local time structures occur repeatedly, and the amplitude of local fluctuations is relatively low. In some balance disorders, characteristic plateau-like structures are observed in the analyzed ASF signal. Additionaly, the amplitude of local fluctuations is higher compared with those of healthy subjects.

3. Angular-segment function parameterization

A number of methods based on the CoP displacement have been used in clinical contexts to examine postural stability. Due to the time-consuming nature of a visual analysis, many techniques are applied to trajectory parameterization. The classical posturographic parameters, most commonly found in the literature, describe the geometry of the trajectory (e.g.

length and area of the trajectory) [10, 11]. Another possibility is to analyze the frequency or time-frequency content of the trajectory components [12, 13]. In some experimental studies, the posturographic signal is analyzed using the fractal theory [14].

In the proposed method, the CoP trajectories are studied as one-dimensional signals that are obtained using the method outlined in Sec. 2. For this reason, it is necessary to define the parameters that characterize the angular-segment function. In this study, three methods are proposed for this purpose.

3.1. Angular-segment function duty coefficient. In this work, a new parameter to quantify human postural stability, the angular-segment function duty coefficient (*DC*), is introduced. The *DC* parameter was designed to detect patients with an increased risk of falling down. The idea arises from the observation that a sudden loss of balance causes a plateau in the angular-segment function. The plateau is relatively easy to detect by calculating the finite differences of the *ASF* (to obtain the signal *ASF'*) and then performing hard thresholding. The hard thresholded signal is *ASF'* if *ASF'* $>$ *THR*, and is 0 if *ASF'* $\leq$ *THR*, where *THR* is the threshold level. In the present work, the threshold level was set to the value that corresponds to 5% of the maximum value of the *ASF'*. In the next step, a sum of the lengths of the non-zero segments is calculated. Finally, the value of the parameter *DC* is calculated as:

$$DC = (1/N) \sum_i L_i, \tag{7}$$

where L_i – length of the i-th segment, N – total length of the angular-segment function (number of signal samples).

3.2. Mean energy per sample. Another parameter proposed in the paper describes the mean energy per sample of the thresholded *ASF'* signal. Because the methods *ASF*α and *ASF*β generate signals of different lengths, the signal energy is divided by the length of the signal to find the parameter E:

$$E = (1/N) \sum_{i=0}^{N-1} \left(ASF'[i]\right)^2, \tag{8}$$

where *ASF'*$[i]$ – samples of the thresholded version of the signal *ASF'*, N – length of the signal (number of signal samples).

3.3. Hurst exponent. Many different parameterization methods based on the displacement of the CoP have been proposed in literature [1, 2]. An interesting framework for studying postural stability is presented in [10, 14]. The underlying idea of this approach is to model the stabilogram as the fractional Brownian motion (fBm). The fractional Brownian motion is a generalization of the well-known ordinary Brownian motion [15]. The fBm is a continuous Gaussian process, which is characterized by a single parameter H, called the Hurst exponent, that is in the range of 0 to 1. The value $H < 0.5$ corresponds to antipersistent motion, where the process has a tendency to turn back upon itself. $H = 0.5$ corresponds to the standard Brownian motion. When the parameter $H > 0.5$, fBm is persistent. This means that the motion has a tendency to continue movement in the same direction.

Many approaches can be used to determine the value of the Hurst exponent. The relevant background information on the topic is presented in [15, 16]. One of the most important properties of fBm is its "self-similarity", which means that any portion of a given fBm can be viewed from a statistical point of view as a scaled version of a larger part of the same realization. Due to the self-similarity properties of fBm, an intuitive approach is to analyze this process using time-scale methods. An obvious way of performing such an analysis is to use a wavelet transform. As was shown in [15], the value of the Hurst exponent can be obtained by carrying out the discrete wavelet transform of an analyzed signal and calculating the slope of the variance plotted as a function of scale in a log-log plot

$$\log_2 \left(var(d_{j,k})\right) = (2H + 1)\, j + C, \tag{9}$$

where j – decomposition level, $d_{j,k}$ – detail coefficients, C – constant that depends on the wavelet.

In this study, a six-level discrete decomposition with a Daubechies wavelet of the order 6 was used to determine the detail coefficients. Moreover, the linear least squares fitting technique was applied to find the best fitting straight line through a set of points in the log-log plot.

In a commonly used approach, the Hurst parameter is calculated separately for the directions ML and AP [1]. For this reason, the trajectory is described by two values, which causes a problem with the interpretation of the result. In the proposed method, the problem is solved by using *ASF*.

4. Results

A static force testing platform, designed and made at the Institute of Electronics, Silesian University of Technology, was used to record ground reaction forces [2]. The signals were processed on a PC connected to the platform. The signals were sampled at 20 ms intervals and the data for each postural task were collected over 30 s. The subjects stood barefoot in an upright position with their eyes open.

Posturographic examinations were performed in three groups. The first group (HS) included 32 young, healthy subjects. Children aged between 10 and 15 years, who suffered from scoliosis (Cobb's angle between 2 and 3), were in the second group (SS). The last group (DBS) consisted of 30 patients exhibiting some disturbances of balance.

STATISTICA (StatSoft, USA) software was used for statistical analysis. In order to evaluate the normality of the distribution, the Kolmogorov-Smirnov and Shapiro-Wilk tests were performed. The Student's unpaired t-test (for equal variances) and Cochran-Cox (for unequal variances) were used to determine significant differences between the pairs of means. The statistical significance level was established at $P < 0.05$.

4.1. Comparison of the methods used for angular-segment function generation. The influence of different methods of *ASF* function generation (*ASF*α and *ASF*β) on the parameters value is given in Table 1. The "+" sign indicates that there

is no significant difference between the means (at statistical significance level of 0.05).

Table 1
The influence of the angular-segment function generation method on the parameter values

Group	Parameter		
	DC	*E*	*H*
HS	−	−	+
DBS	−	−	−
SS	+	+	+

As we can see, there are no significant differences between the mean values of the parameters generated using both methods for the scoliosis group (SS). This is because the analyzed trajectories in that group were similar to each other. A low intergroup variability was observed for selected patients with scoliosis (Cobb's angle between 2 and 3). In other cases, the parameter values generally depended on the method of angular-segment function generation.

4.2. Discriminative potential of parameters. In order to examine the discriminative potential of the parameters, a statistical hypothesis test for an equality of mean values was performed. The obtained results are shown in Table 2. The "–" sign indicates that there is a significant difference between the means.

Table 2
The discriminative potential of the parameters

Group	DBS		SS	
	$ASF\alpha$	$ASF\beta$	$ASF\alpha$	$ASF\beta$
HS	H – DC – E –	H – DC – E –	H – DC – E +	H – DC – E +
DBS			H – DC – E –	H + DC – E –

The analysis of the human postural stability using the parameter *DC* shows very promising results. Regardless of the method used to generate angular-segment function, statistically significant differences were found between the mean values of the parameter for each group.

In the case of the method $ASF\alpha$, the results obtained for the Hurst parameter showed significant differences between the mean values of the parameter. On the basis of the parameter H, we are able to distinguish healthy subjects (HS) from the subjects with a scoliosis (SS) and from the patients exhibiting some disturbances of balance (DBS). There were no significant differences between the mean values of the parameter calculated for patients with a disturbance of balance (DBS) and scoliosis (SS) for the method $ASF\beta$.

The parameter E does not allow the subjects to be properly distinguished. There are no significant differences between the mean values of the parameter E observed in the groups HS and SS. This phenomenon occurs in both methods – $ASF\alpha$, $ASF\beta$. Thus, we are not able to distinguish healthy subjects from patients with scoliosis based on the parameter E.

4.3. Reliability of parameters. The reliability of different parameterization methods was studied by deriving the relative dispersion of the parameters, *RD*, defined as a ratio between the standard deviation and the mean for each group. The calculations were performed for both methods – $ASF\alpha$ and $ASF\beta$. Table 3 summarizes the results.

A reliable parameter is characterized by a low value of *RD*. Among the parameters, *DC* is the most reliable one, while E is relatively stable. The value *RD* of the Hurst exponent exhibits a relatively low reliability.

The high reliability of the parameter *DC* is proved by the low value of the relative dispersion. The value of relative dispersion was smaller than *RD* calculated for the parameters H and E in all cases. The deterioration of the *DC* reliability in the DBS group results from the fact that the geometry of the trajectories can differ remarkably from each other.

In each case, the relative dispersion of the parameter E was smaller than *RD* calculated for the Hurst exponent. However, by comparing the relative dispersion of *DC* to the relative dispersion of the parameter E, it is clear that *DC* provides better selectivity.

Table 3
The basic statistical parameters

Group	Parameter					
	DC		*E*		*H*	
	$ASF\alpha$	$ASF\beta$	$ASF\alpha$	$ASF\beta$	$ASF\alpha$	$ASF\beta$
HS	m= 0.815 std= 0.021 std/m=0.0258	m= 0.833 std= 0.0196 std/m=0.0235	m= 3.0 std= 0.374 std/m=0.125	m= 3.504 std= 0.355 std/m=0.101	m= 0.236 std= 0.048 std/m=0.203	m= 0.227 std= 0.052 std/m=0.229
DBS	m= 0.556 std= 0.08 std/m=0.144	m= 0.621 std= 0.063 std/m=0.1014	m= 2.12 std= 0.427 std/m=0.201	m= 2.657 std= 0.348 std/m=0.131	m= 0.245 std= 0.068 std/m=0.277	m= 0.184 std= 0.08 std/m=0.435
SS	m= 0.793 std= 0.044 std/m=0.055	m= 0.806 std= 0.034 std/m=0.0422	m= 3.21 std= 0.744 std/m=0.232	m= 3.7 std= 0.7 std/m=0.189	m= 0.187 std= 0.07 std/m=0.374	m= 0.182 std= 0.045 std/m=0.247

The information provided by the Hurst exponent seems to be uncertain, so we were unable to attach any great diagnostic significance to the Hurst exponent. This opinion is shared by other authors [11]. However, we must emphasize that in the proposed approach, we analyzed the segment function using the fractional Brownian motion. In many papers the fBm technique is used separately for directions AP and ML [10, 14].

Generally, a lower value of the relative dispersion is observed for the method $ASF\beta$. This dependence is preserved for two parameters – DC and E. However, it does not hold for the Hurst exponent.

5. Conclusions

In this paper, we propose a method for the characterization of stabilograms using the angular-segment function. In contrast to classical methods of analysis where postural stability is quantified in terms of geometric properties of the stabilogram (e.g. length and area of the stabilogram), the proposed approach is based on a different technique. It has been shown that the CoP trajectory can be described in an alternative way, using a one-dimensional angular-segment function. The obtained results confirm that this function is a valuable tool in the characterization of stabilographic trajectories. It is also worth noting that the proposed method reduces dimensionality of the problem.

In Sec. 2 we provide a detailed description of the two algorithms used to determine the angular-segment function. The first variant, named $ASF\alpha$, assumes the constant distance between recalculated trajectory points, while the second, $ASF\beta$, assumes a constant path length along the trajectory.

In the paper, special attention has been paid to the development of the methods for the parameterization of the angular-segment function. For this reason, we proposed three parameters: DC, E, H. A detailed study was performed to explore the discriminative potential and reliability of the proposed parameters. As it has been shown, among the parameters, the parameter DC offers the best performance by delivering a high discriminative potential and high reliability. Moreover, the influence of the methods used to generate the angular-segment function on the parameterization result has been examined.

REFERENCES

[1] D.A. Winter, "Human balance and posture control during standing and walking", *Gait and Posture* 3, 193–214 (1995).

[2] Z. Kidoń, "Digital signal processing of stabilographic signals" ("Cyfrowe przetwarzanie sygnałów stabilograficznych"), *PhD Thesis*, Silesian University of Technology, Gliwice, 2003, (in Polish).

[3] D.A. Winter, *Biomechanics and Motor Control of Human Movement*, Wiley, London, 2009.

[4] FB. Horak, "Clinical assessment of balance disorders", *Gait and Posture* 7, 76–84 (1997).

[5] M. Salavati, M.R. Hadian, and M. Mazaheri, "Test–retest reliabty of center of pressure measures of postural stability during quiet standing in a group with musculoskeletal disorders consisting of low back pain, anterior cruciate ligament injury and functional ankle instability", *Gait and Posture* 29, 460–464 (2009).

[6] Z. Kidoń, D. Kania, J. Fiołka, and K. Pethe-Kania, "Stabilographic stand for diagnosis of patiens after a hip replacement surgery", *Electeronics – Constructions, Technologies, Applications* 11, CD-ROM (2008), (in Polish).

[7] K. Pethe-Kania, Z. Kidoń, and D. Kania, "Modern method of the progress estimation in rehabilitation of patients after hip replacement surgery", *Rehabilitation* 4, 41–44 (2007), (in Polish).

[8] K. Pethe-Kania, "Stabilography in the rehabilitation of patients after a hip replacement arthroplasty", *PhD Thesis*, Medical University, Katowice, 2011, (in Polish).

[9] C.T. Zahn and R.Z. Roskies, "Fourier descriptors for plane closed curves", *IEEE Trans. Computers* C-21 (3), 269–281 (1972).

[10] L. Baratto, P.G. Morasso, C. Re, and G. Spada, "A new look at posturographic analysis in the clinical context: sway-density vs. other parameterization techniques", *Motor Control* 6 (3), 246–270 (2002).

[11] J.A. Raymakers, M.M. Samson, and H.J.J. Verhaar, "The assessment of body sway and the choice of the stability parameter(s)", *Gait and Posture* 21, 48–58 (2005).

[12] M. Ferdjallah, G.F. Harris, and J.J. Wertch, "Instantaneous postural stability characterization using time-frequency analysis", *Gait and Posture* 10, 129–134 (1999).

[13] J. Fiołka, "Postural stability analysis: a wavelet based approach", *Proc. Int. Conf. on Signals and Electronics Systems* 1, CD-ROM (2010).

[14] J.J. Collins and C. De Luca, "Open-loop and closed-loop control of posture: a random-walk analysis of center-of-pressure trajectories", *Experimental Brain Research* 95, 308–318 (1993).

[15] P. Flandrin, "Wavelet analysis and synthesis of fractional brownian motion", *IEEE Trans. on Information Theory* 38 (2), CD-ROM (1992).

[16] P.S. Addison, *The Illustrated Wavelet Transform Handbook*, Institute of Physics Publishing, Bristol, 2002.